

Experimental investigation of bidirectional series resonant DC-DC converter in different operating modes

Angel Lichev, Yassen Madankov, Vasil Mihov

Department of Electrical Engineering and Electronics, Faculty of Technical, University of Food Technologies, Plovdiv, Bulgaria

Article Info

Article history:

Received Jun 16, 2023

Revised Oct 24, 2023

Accepted Nov 7, 2023

Keywords:

Bidirectional energy flow
Phase-shift control
Resonant DC-DC converter
Soft commutation
ZVS

ABSTRACT

This paper presents a study of bidirectional series resonant DC/DC converter. The main operating modes of the converter with phase-shift control technique are observed. An experimental survey with a laboratory model of such type of converter working over the resonant frequency is made. The functionality of the studied device operating in a wide area of loading is demonstrated with waveforms of the main parameters. The conducted measurements are used to build the experimental output characteristics of the converter. A similarity of the experimental results with the theoretical are denoted, and the ability to achieve current source characteristics for the whole range of loading is proven. The possibility of the studied converter for operation both in forward and reverse modes of energy flow is proved, which positions the device as an appropriate variant for implementation in the storage system control area.

This is an open access article under the [CC BY-SA](https://creativecommons.org/licenses/by-sa/4.0/) license.



Corresponding Author:

Angel Lichev

Department of Electrical Engineering and Electronics, Faculty of Technical

University of Food Technologies

26 Maritza Blvd., Plovdiv 4002, Bulgaria

Email: angel_lichev@abv.bg

1. INTRODUCTION

The 2030 agenda for sustainable development, in particular goal 7, requires all member states of the United Nations to implement programs that stimulate the expansion of renewable energy sources. That is one of the reasons why the investment in green power has grown in the past few years [1]–[4]. Nevertheless, in rural areas where direct access to the power grid is not common, renewable energy could be one of the suitable solutions. A considerable shortcoming, in this case, is production intermittency, which is particularly marked in photovoltaic (PV) and wind power plants [5], [6].

Therefore, hybrid power generation systems become more common [7]–[11]. To increase the system efficiency, battery storage technologies are implemented [12]. In such a way, during an energy production peak, the surplus of energy could be stored, and when the generation becomes lower than the consumption this energy could be reverse feeding into the main supply. Wherever necessary, the shortfall in energy could be compensated by the batteries. Obviously, in this case, a bidirectional transfer of the power is required.

The current of the batteries has to be controlled during the charging (discharging) process [13]. Exceeding it reduces the battery life and could cause accidents. Therefore, power converters must ensure smooth control of the output current value. A good solution, in this case, is the bidirectional resonant converters [14]–[18]. It is well known that resonant circuit ensures soft commutation capability, thus improving its efficiency and the efficiency of the whole system [19]–[22].

Lichev [23] presented a study of inductor-capacitor or LC bidirectional series resonant DC-DC converter. Unlike inductor-inductor-capacitor or LLC converters [24], [25] the resonant tank circuit consists of only two reactive elements. This creates an opportunity for converter size optimization, which leads to

weight and cost reduction. Furthermore, the studied topology provides bidirectional energy transfer and enables a soft commutation operation. This makes bidirectional series resonant DC-DC converters a proper solution for battery charging applications.

The results from the theoretical study in [23] show that the analysed converter operates with no limitations in zero voltage switching (ZVS) irrespective of the control parameter value. The characteristics of the converter are like those of a perfect current source. The value of the output voltage is greater than that of the input voltage. This paper expands the research of the converter supplementing experimental examinations and achieving results that approve the functionality of the design.

2. CONVERTER ANALYSIS

The circuit diagram of the studied converter as seen in Figure 1. is composed of two fully controlled inverter-rectifier semiconductor H-bridges. Each of them is composed of four transistors with reverse diodes, as well as snubber capacitors for reduction of the commutation losses. The energy transmission is through the serial resonant tank, inductor L_r and capacitor C_r .

The advantages of high-frequency operation are well known. Possible converter operating modes when working over the resonant frequency are explored in detail in [23]. The energy flow could be in a forward direction (from U_d to U_0), as well as in a reverse direction (from U_0 to U_d), depending on the value of the selected control parameter. These circuit characteristics give the opportunities for the realization of reversible supply device which can achieve smoothly energy flow direction change. Depending on flow direction each of the H-bridge stages could operate either as an inverter or as a rectifier. Conditionally is assumed that the left side of the circuit is an input stage with input parameters U_d and i_d , and the right one is output – U_0 is defined as an output voltage, i_0 – output current.

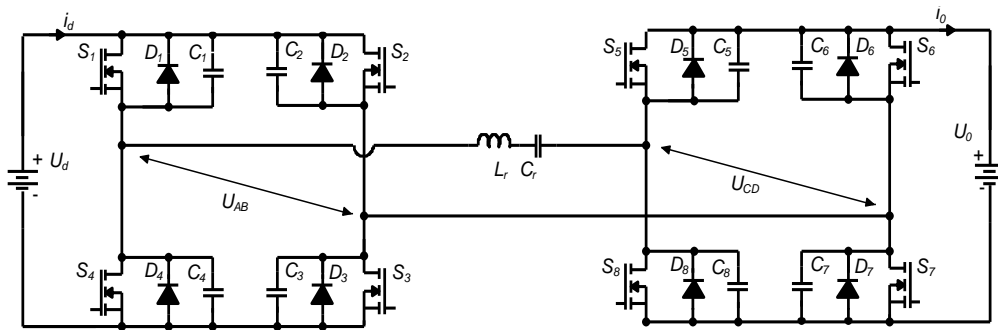


Figure 1. Circuit diagram of the converter

Waveforms of the main electrical parameters of the converter are shown in Figures 2 and 3. The inductor current is denoted with i_L , the resonant capacitor voltage – with u_C , and the voltages on the input and output side of the LC circuit – with u_{AB} and u_{CD} . During the forward operation mode, the input semiconductor H-bridge is supplied with the DC voltage U_d and the average value of currents i_d and i_0 are in the “forward” direction. So, i_d flows from supply U_d , through the input bridge which works as an inverter, to the resonant circuit. The output current i_0 direction is through the output bridge (rectifier) to the load. Vice versa, in reverse mode the output stage behaves like an inverter which supplies a resonant tank from voltage U_0 and current i_0 , and the input stage – as a rectifier, feeding back energy to supply. The two-way energy transmission in each of the mentioned modes is achieved via reverse diodes D_1 - D_8 .

The current through the inductor i_L lags from the input H-bridge’s voltage u_{AB} at angle φ because the operating frequency is greater than the resonant frequency. This is the time for conducting of the input transistors S_1 - S_4 . Transistors of the output stage S_5 - S_8 begin to conduct every time when i_L reaches zero value. This way they operate in soft commutation mode. Output transistors are active up to the moment of u_{CD} polarity change.

Semiconductor elements of the output H-bridge switch after a time corresponding to the angle δ . In this way, controlling the phase shift between u_{AB} and u_{CD} , the power control is realized. According to the studies made in [23], this method is concluded as an optimal for control. A phase plane method for analyzing the process in the converter is proposed in [23], where the following assumptions are made to accomplish simplification of the mathematical equations: i) It is assumed that all elements of the converter circuit are ideal; ii) The impact of the ($C_1 - C_8$) snubbers is neglected; and iii) Pulsations of U_d and U_0 voltages are neglected, so the voltages of the two inverter bridges – u_{AB} and u_{CD} , are ideal square waves.

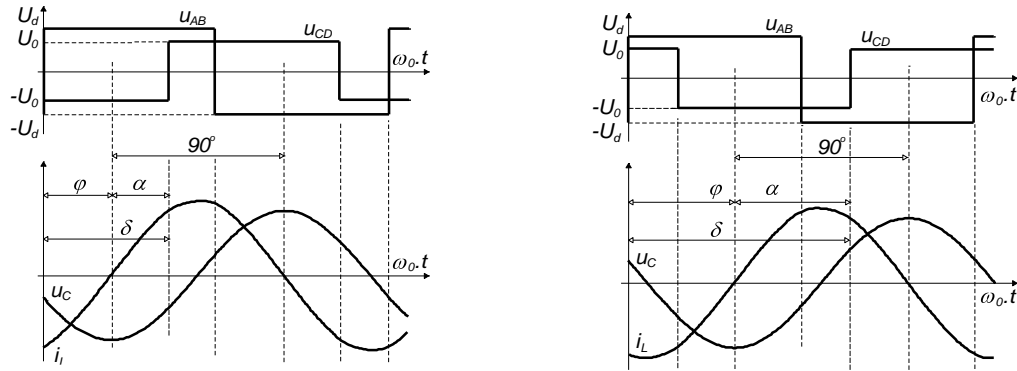


Figure 2. Waveforms of the converter at forward mode Figure 3. Waveforms of the converter at reverse mode

According to these assumptions, the resonant tank frequency, the characteristic impedance and the ratio of the frequencies could be obtained as (1)-(3):

$$f_0 = \frac{1}{2\pi\sqrt{L.C}} \tag{1}$$

$$Z_0 = \sqrt{\frac{L}{C}} \tag{2}$$

$$\nu = \frac{f_s}{f_0} \tag{3}$$

In order to achieve more generalized results from the analysis all parameters are normalized – voltages relative to U_d , and the current to U_d/Z_0 . The control range of the converter (angle δ) is limited to the interval from 90° to 270° because in these borders it has a possibility for operation in the whole loading area without violating the soft commutation conditions. The output characteristics of such kind of converter with the relevant control method are presented in Figure 4. They are achieved at normalized frequency $\nu = 1.15$. The output characteristics show that the converter operates as a perfect current source.

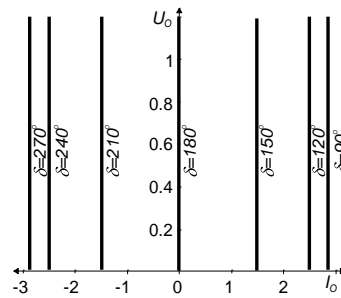


Figure 4. Output characteristics of the converter (control parameter – δ)

3. EXPERIMENTAL RESULTS

Using the methodology described in research [23], a series resonant DC-DC converter with the relevant nominal parameters is designed: output power – $P_{ON} = 200 \text{ W}$; input voltage – $U_{dN} = 100 \text{ V}$; output voltage – $U_{oN} = 100 \text{ V}$; switching frequency – $f_{SN} = 50 \text{ kHz}$; normalized frequency – $\nu_N = 1.15$. Values $L_r = 531.8 \mu\text{H}$; $C_r = 25.36 \text{ nF}$ are calculated for resonant tank parameters. Figure 5 shows a fully functional model of the designed converter. The commutation of the power switches is based on a microcontroller ZF083 A, which provides 3.5 V square wave control pulses that are phase shifted on angle δ . Since the 3.5 V magnitude is not high enough, the signal is amplified to 15 V, then applied to ZVS drivers and the two H-bridge stages. The input and output voltages and currents are measured by digital multimeters. Regarding the data received, the output characteristics of the converter are built.

Studies with different values of the supply voltage U_d from the battery block have been conducted. In order to cover the work of the converter in the whole area of the output characteristics a battery block is also attached on the load side. This gives the opportunity to study the operating modes, as well as the work of the

converter in buck and boost modes. Different operating frequencies in the range $f_s = 46\div 59$ kHz have been tested. The main part of the accomplished results is at a frequency which is close to the designed $f_s = 50$ kHz ($v_N = 1.154$).

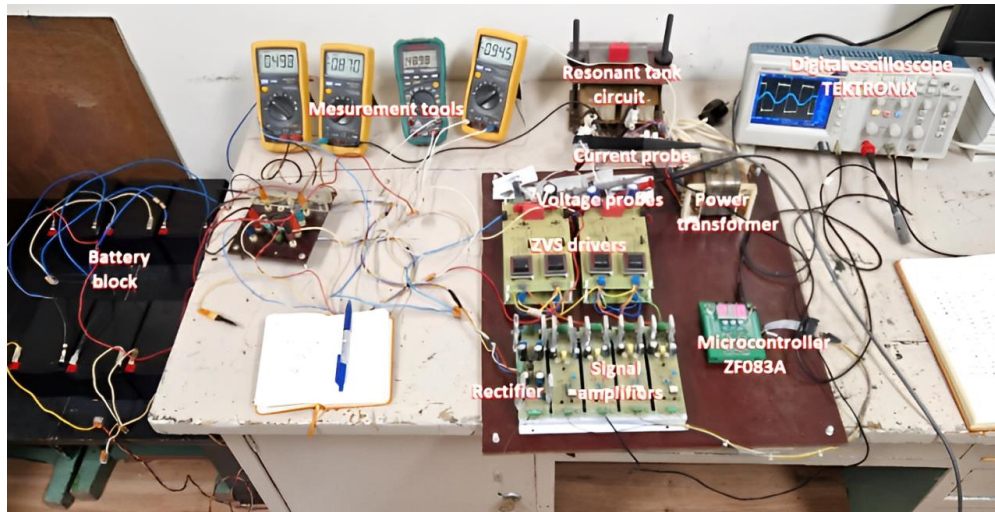


Figure 5. A laboratory model of the DC/DC converter

3.1. Waveforms of the converter

Waveforms showing the work of the converter at a settled regime are demonstrated in Figure 6. Both of the figures show the square wave voltage u_{AB} at the input bridge output and the current through the resonant inverter i_L . Figure 6(a) demonstrates the forward mode at phase shift angle $\delta = 90^\circ$, and Figure 6(b) at maximal power feed-back from “load” to supply ($\delta = 270^\circ$).

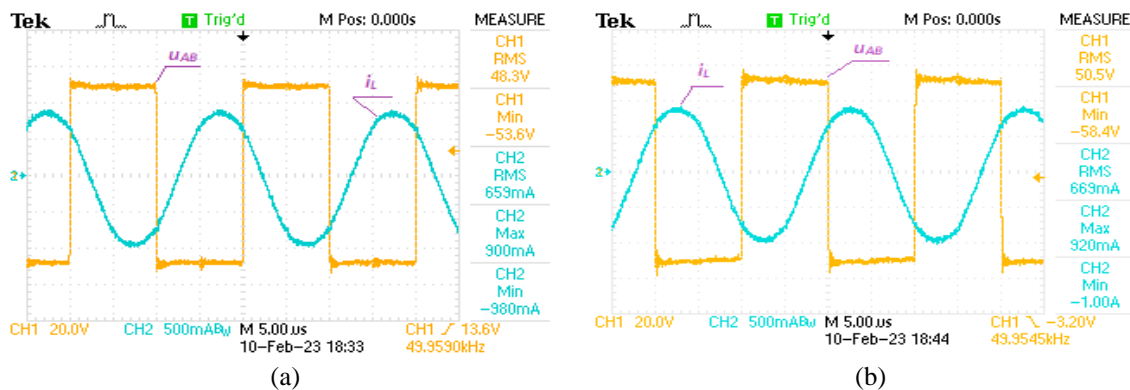


Figure 6. Waveforms of voltage u_{AB} and i_L at (a) forward mode and (b) reverse mode

Figure 7 demonstrates the voltages on both sides of the resonant tank (u_{AB} and u_{CD}) in boost mode Figure 7(a) and in buck mode of the converter Figure 7(b). In this figure, the current through one diagonal of the input H-bridge’s transistors is also shown. From these waveforms, the conducting periods of the input stage power switches are distinctly visible. The two figures are also in the two modes of operation – forward and reverse with the same controlling angles δ .

Waveforms of the resonant current i_L at different operating frequencies ($f_s = (46, 50, 59)$ kHz) are shown in Figure 8(a). They are taken in forward mode at $\delta = 90^\circ$. It is known that for such kind of converter at frequencies closer to the resonant one, higher energy transfer can be obtained. From the illustration can be noted that the current rises significantly for lower frequencies and with that the delivered power. Figure 8(b) demonstrates the soft commutation during the process of a transistor switch-on.

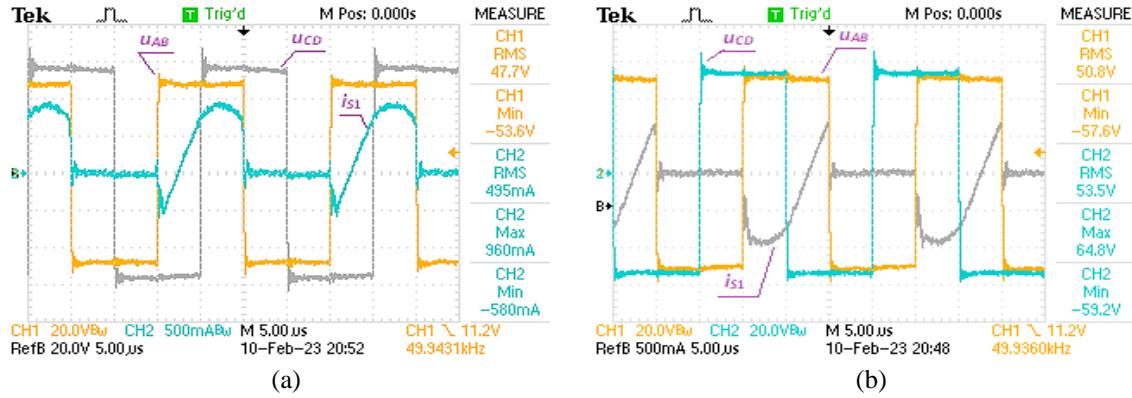


Figure 7. Oscilloscope waveforms of converter voltages u_{AB} and u_{CD} and the current through input H-bridge semiconductor switches i_{s1} (a) boost mode and (b) buck mode

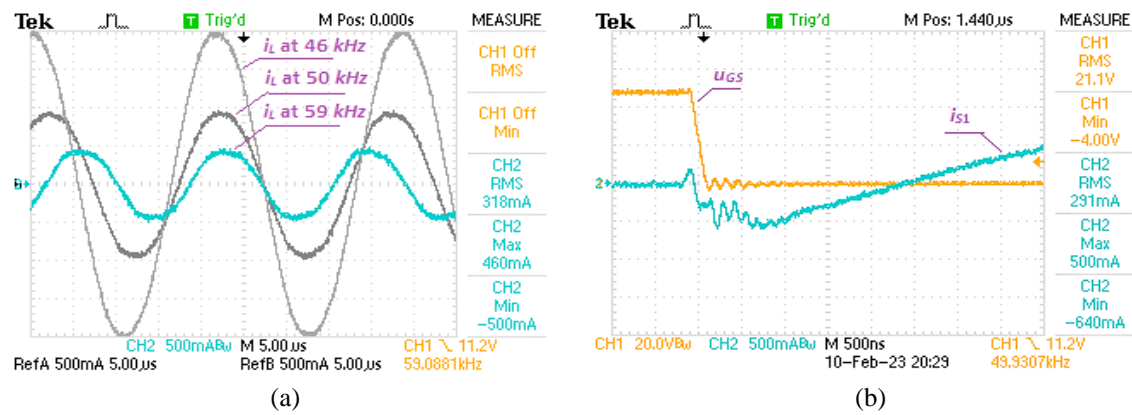


Figure 8. Waveforms of (a) current through the resonant tank i_L and (b) drain-source voltage u_{DS} and source current i_{s1} of transistor

3.2. Output characteristics

Experimental measurements of the converter operating parameters at the selected working frequency have been conducted. They are made at different values of the control parameter δ . Figure 9 presents the converter experimental output characteristics based on the results obtained in Table 1. The study has been conducted at input voltage $U_d = 48$ V, which is provided from a battery block. On the output of the converter is also a battery block whose voltage is changed in the range $U_0 = 12\text{--}50$ V.

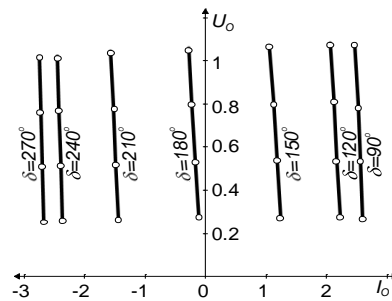


Figure 9. Experimentally obtained normalized output characteristics of the converter

The frequency is $f_{SN} = 50$ kHz. The output characteristics are transformed in normalized values. Current limiting with the increase of the voltage is observed which differs from the theoretical characteristics in Figure 4. The main reason for this is the assumptions for element ideality in the mathematical equations in the analysis.

Table 1. Experimental measurements of the resonant DC/DC converter

δ	U_d	I_d	U_0	I_0	δ	U_d	I_d	U_0	I_0
90°	47.7	0.258	12.51	0.862	210°	47.8	-0.076	12.47	-0.474
	47.6	0.496	25.19	0.849		48.0	-0.184	24.84	-0.49
	47.7	0.716	37.28	0.836		48.2	-0.296	37.42	-0.506
	47.6	0.947	50.11	0.816		48.5	-0.404	49.42	-0.523
120°	47.6	0.243	12.76	0.739	240°	47.9	-0.161	12.35	-0.781
	47.6	0.447	25.30	0.72		48.2	-0.352	24.60	-0.794
	47.5	0.661	38.30	0.702		48.4	-0.545	37.17	-0.809
	47.6	0.850	50.28	0.684		48.8	-0.726	48.98	-0.825
150°	47.6	0.160	12.71	0.413	270°	48.0	-0.198	12.08	-0.886
	47.7	0.284	25.24	0.393		48.3	-0.423	24.52	-0.899
	47.6	0.409	38.15	0.373		48.5	-0.692	37.03	-0.911
	47.9	0.518	50.15	0.354		48.9	-0.863	48.73	-0.927
180°	47.8	0.043	12.60	-0.033					
	47.8	0.045	25.06	-0.052					
	47.9	0.037	37.84	-0.071					
	48.2	0.035	49.90	-0.089					

4. CONCLUSION

The presented study describes the operating modes of bidirectional series resonant DC-DC converter. A laboratory model of the converter is designed and developed. Series of experimental investigations which demonstrate its functionality for the whole range of the expected working area have been conducted. The results have proven the ability of such resonant converter controlled with the described phase-shift method to work in both operating modes – forward and reverse, as well as in buck and boost regimes. The experimental output characteristics are obtained and similarity with the theoretical characteristics is demonstrated. The possibility to reverse the direction of the energy from the supply to the load and vice versa makes the converter suitable for implementation in the vast growing area of electrical storage systems. The specific characteristics, similar to an ideal current source and the opportunity for smooth control of the power flow magnitude and direction place the converter in a good position as a battery charging module.

ACKNOWLEDGEMENTS

We express our gratitude to the government-funded program "Young Scientists and Postdoctoral Researchers – 2" for their grant of 300 EUR, which supported our publication efforts.




REFERENCES

- [1] R. M. Reffat and R. Ezzat, "Impacts of design configurations and movements of PV attached to building facades on increasing generated renewable energy," *Solar Energy*, vol. 252, pp. 50–71, 2023, doi: 10.1016/j.solener.2023.01.040.
- [2] P. R. Kumar and R. Padma, "A Novel Control Method for Integration of Battery Energy Storage System in Microgrid for Energy Management System," *International Journal of Innovative Technology and Exploring Engineering*, vol. 9, no. 2, pp. 4974–4977, 2019, doi: 10.35940/ijitee.b9079.129219.
- [3] N. M. Kumar, S. S. Chopra, A. A. Chand, R. M. Elavarasan, and G. M. Shafiullah, "Hybrid Renewable Energy Microgrid for a Residential Community: A Techno-Economic and Environmental Perspective in the Context of the SDG7," *Sustainability*, vol. 12, no. 10, p. 3944, May 2020, doi: 10.3390/su12103944.
- [4] J. Lee and J. Won, "Multifunctional Onboard Charger for Electric Vehicles Integrating a Low-Voltage DC-DC Converter and Solar Roof," *IEEE Journal of Emerging and Selected Topics in Power Electronics*, 2023, doi: 10.1109/JESTPE.2023.3309974.
- [5] K. Jm, S. Sheik Mohammed, T. P. I. Ahamed, and M. Shafeeque, "Design and Simulation of Stand-alone DC Microgrid with Energy Storage System," *IEEE International Conference on Intelligent Techniques in Control, Optimization and Signal Processing, INCOS 2019*, 2019, doi: 10.1109/INCOS45849.2019.8951384.
- [6] A. Saha, S. Misra, and P. M. Progya, "Design and simulation based stand-alone solar micro grid system for island areas," *2019 5th International Conference on Advances in Electrical Engineering, ICAEE 2019*, pp. 229–234, 2019, doi: 10.1109/ICAEE48663.2019.8975488.
- [7] Z. Ma, F. Dong, J. Wang, Y. Zhou, and Y. Feng, "Optimal design of a novel hybrid renewable energy CCHP system considering long and short-term benefits," *Renewable Energy*, vol. 206, pp. 72–85, 2023, doi: 10.1016/j.renene.2023.02.014.
- [8] B. Zhao, Q. Yu, and W. Sun, "Extended-phase-shift control of isolated bidirectional DC-DC converter for power distribution in microgrid," *IEEE Transactions on Power Electronics*, vol. 27, no. 11, pp. 4667–4680, 2012, doi: 10.1109/TPEL.2011.2180928.
- [9] M. A. Obaidah, F. Soroni, and M. M. Khan, "Development of a Hybrid Power Generation System," in *2021 IEEE 12th Annual Ubiquitous Computing, Electronics & Mobile Communication Conference (UEMCON)*, Dec. 2021, pp. 0717–0722, doi: 10.1109/UEMCON53757.2021.9666682.
- [10] H. Zhang, Y. Wang, H. Yu, and Z. Chen, "A Novel Flexible Multiport Interlinking Converter for DC Microgrid Clusters," *IEEE Transactions on Industry Applications*, 2023, doi: 10.1109/TIA.2023.3322981.
- [11] P. Roy, J. He, T. Zhao, and Y. V. Singh, "Recent Advances of Wind-Solar Hybrid Renewable Energy Systems for Power Generation: A Review," *IEEE Open Journal of the Industrial Electronics Society*, vol. 3, pp. 81–104, 2022, doi: 10.1109/OJIES.2022.3144093.
- [12] S. Supanyapong, W. Pattarapongsathit, A. Billsalam, D. Guilbert, and P. Thounthong, "Averaged large-signal model of a DC-DC isolated forward resonant reset converter for a solar cell battery charger using internet of things: implementation," *International*




- Journal of Power Electronics and Drive Systems*, vol. 13, no. 3, pp. 1732–1747, 2022, doi: 10.11591/ijpeds.v13.i3.pp1732-1748.
- [13] W. Xiong, Z. Yan, D. Tang, W. Zhou, and R. Mai, "A Hybrid Topology IPT System with Partial Power Processing for CC-CV Charging," *IEEE Transactions on Power Electronics*, 2023, doi: 10.1109/TPEL.2023.3310713.
- [14] Y. Yuan, T. Tao, Y. Huang, N. Peng, W. Liu, and G. Xing, "A High-Gain Five-Bridge-Arms Bidirectional DC-DC Converter for Wide Range Applications," *IEEE Journal of Emerging and Selected Topics in Power Electronics*, 2023, doi: 10.1109/JESTPE.2023.3324212.
- [15] R. M. Reddy and M. Das, "Reconfigurable Resonant DC-DC Bidirectional Converter for Wide Output Voltage Applications," *IEEE Transactions on Industry Applications*, pp. 1–10, 2023, doi: 10.1109/tia.2023.3314010.
- [16] F. Yuan, R. Hao, X. You, and P. Xiang, "A High Voltage Gain Soft-Switching Bidirectional DC-DC Converter With Wide Range Using Resonant Network," *IEEE Transactions on Power Electronics*, 2023, doi: 10.1109/TPEL.2023.3309012.
- [17] N. Hinov and T. Grigorova, "Design Considerations of Multi-Phase Buck DC-DC Converter," *Applied Sciences (Switzerland)*, vol. 13, no. 19, 2023, doi: 10.3390/app131911064.
- [18] D. Mou *et al.*, "Overview of Multi-Degree-of-Freedom Modulation Techniques for Dual Active Bridge Converter," *IEEE Journal of Emerging and Selected Topics in Power Electronics*, 2023, doi: 10.1109/JESTPE.2023.3323288.
- [19] M. Pastor, J. Dudrik, and A. Marcinek, "Optimization of Soft-Switching DC-DC Converter," *2023 International Conference on Electrical Drives and Power Electronics, EDPE 2023 - Proceedings*, 2023, doi: 10.1109/EDPE58625.2023.10274020.
- [20] B. T. Kadhem, S. S. Harden, and K. M. Abdhassan, "High-performance Cuk converter with turn-on switching at zero voltage and zero current," *Bulletin of Electrical Engineering and Informatics*, vol. 12, no. 3, pp. 1359–1370, 2023, doi: 10.11591/eei.v12i3.4499.
- [21] M. A. N. Kasiran, A. Ponniran, N. N. M. Siam, M. H. Yatim, N. A. C. Ibrahim, and A. Md Yunos, "DC-DC converter with 50 kHz–500 kHz range of switching frequency for passive component volume reduction," *International Journal of Electrical and Computer Engineering*, vol. 11, no. 2, pp. 1114–1122, 2021, doi: 10.11591/ijece.v11i2.pp1114-1122.
- [22] Z. M'barki, K. S. Rhazi, and Y. Mejdoub, "A novel fuzzy logic control for a zero current switching-based buck converter to mitigate conducted electromagnetic interference," *International Journal of Electrical and Computer Engineering*, vol. 13, no. 2, pp. 1423–1436, 2023, doi: 10.11591/ijece.v13i2.pp1423-1436.
- [23] A. Lichev, "Modeling and Optimization of Bidirectional Dual Active Bridge DC-DC Converter Topologies." Department Electrical and Electronics, UFT Plovdiv, UFT Plovdiv, Bulgaria, 2018.
- [24] M. Qawaqzeh, R. Zaitsev, O. Miroshnyk, M. Kirichenko, D. Danylchenko, and L. Zaitseva, "High-voltage DC converter for solar power station," *International Journal of Power Electronics and Drive Systems*, vol. 11, no. 4, pp. 2135–2144, 2020, doi: 10.11591/ijpeds.v11.i4.pp2135-2144.
- [25] A. H. M. Dobi and M. R. Sahid, "Non-isolated LLC resonant DC-DC converter with balanced rectifying current and stress," *Indonesian Journal of Electrical Engineering and Computer Science*, vol. 18, no. 2, pp. 698–706, 2020, doi: 10.11591/ijeecs.v18.i2.pp698-706.

BIOGRAPHIES OF AUTHORS






Angel Lichev    works as an assistant professor in the EEE Department at the UFT – Plovdiv, Bulgaria. He received his B.Ec. degree in PU “Paisii Hilendarski” in 2006 and his M.Eng. and Ph.D. degrees in Electrical Engineering from The UFT – Plovdiv, in 2015 and 2018, respectively. Throughout his qualifying, he also works in the sphere of energetics and electrical installation. Apart from the university activities, he is engaged in several projects relating to the practical training of young graduates in the area of electrical engineering and electronics. He works in the field of power converters, control systems, and green energy systems. He can be contacted at email: a_lichev@uft-plovdiv.bg.



Yasen Madankov    works as an assistant professor in EEE Department at the University of Food Technologies – Plovdiv, Bulgaria. He received his B.Eng. and M.Eng. degrees in Automation Engineering from TU – Sofia (Branch Plovdiv), Bulgaria in 2007 and 2009, respectively. While working in the hardware and software development area he finished his Ph.D. study in Industrial Electronics in University of Food Technologies – Plovdiv in 2018. Aside from the university activities he manages projects in renewable energy sources area and especially the PV sector. He works in the field of photovoltaic systems, renewable energy, storage solutions, industrial electronics and embedded systems. He can be contacted at email: y_madankov@uft-plovdiv.bg.



Vasil Mihov    is a lecturer in EEE Department at the University of Food Technologies – Plovdiv, Bulgaria. His B.Eng. and the M.Eng. degrees in electronics are received, both from TU - Sofia (Branch Plovdiv), in 2003 and 2005, and Ph.D. degree in Industrial electronics in 2011. He spent ten years working in several companies, including BTL Industries Ltd. and Elit 95 Ltd. where he participated in various projects related to manufacturing, maintenance and customer support. He returned to the scientific work in 2021 and became an assistant professor in 2022. He works in the field of power electronics, electric drives and alternative energy systems. He can be contacted at email: v_mihov@uft-plovdiv.bg.